

SMR 1331/7

AUTUMN COLLEGE ON PLASMA PHYSICS

8 October - 2 November 2001

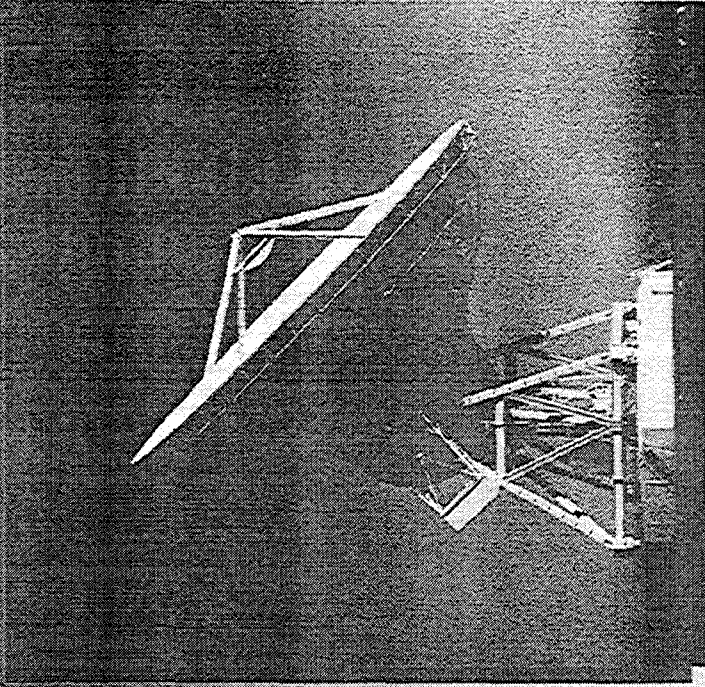
Radioastronomical Diagnostics of Astrophysical Plasma Turbulence

S.R. Spangler

University of Iowa, Dept. of Physics
U.S.A.

These are preliminary lecture notes, intended only for distribution to participants.

Radioastronomical Diagnostics of Astrophysical Plasma Turbulence



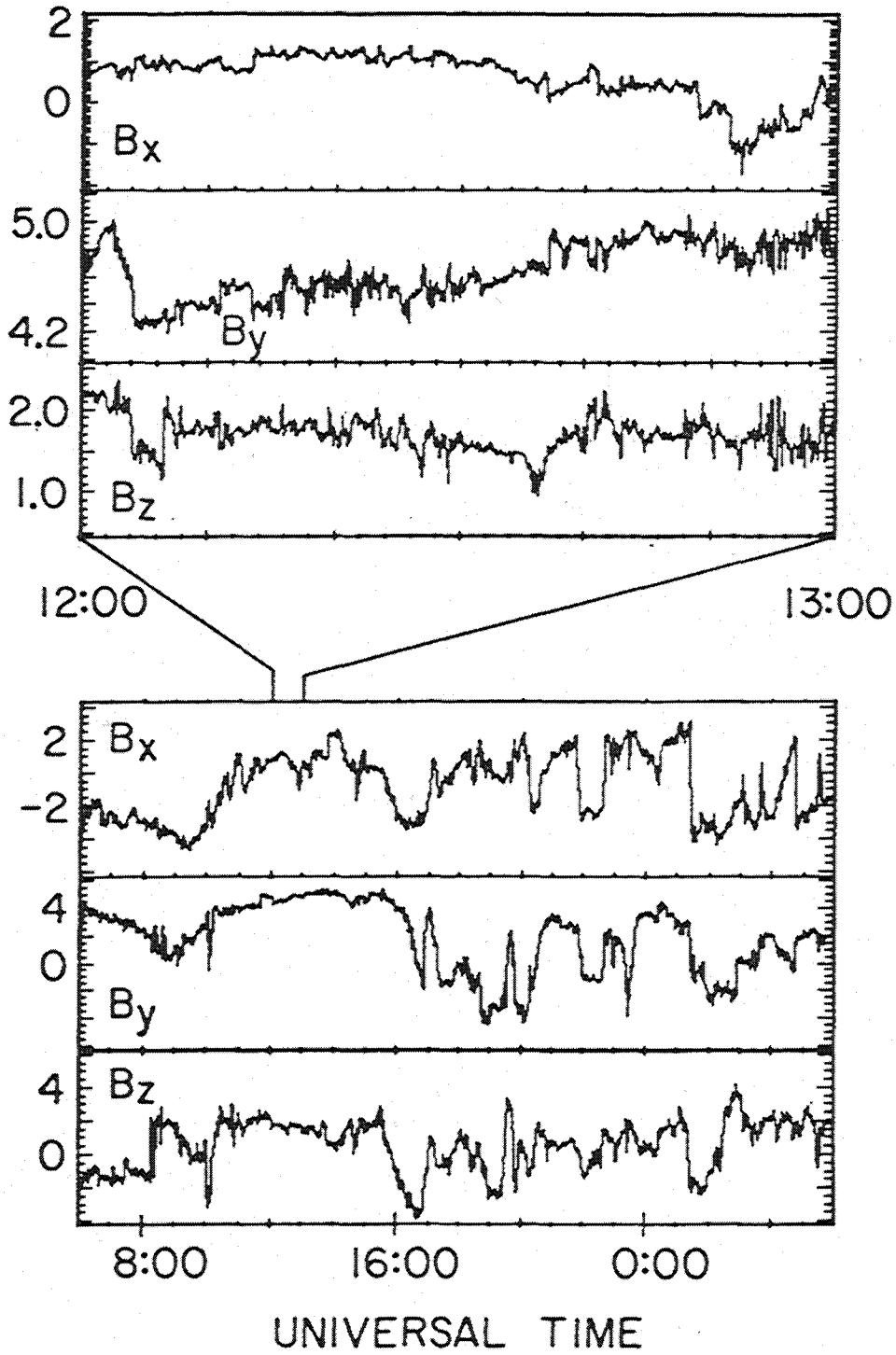
Steven R. Spangler

Department of Physics and Astronomy

University of Iowa, USA

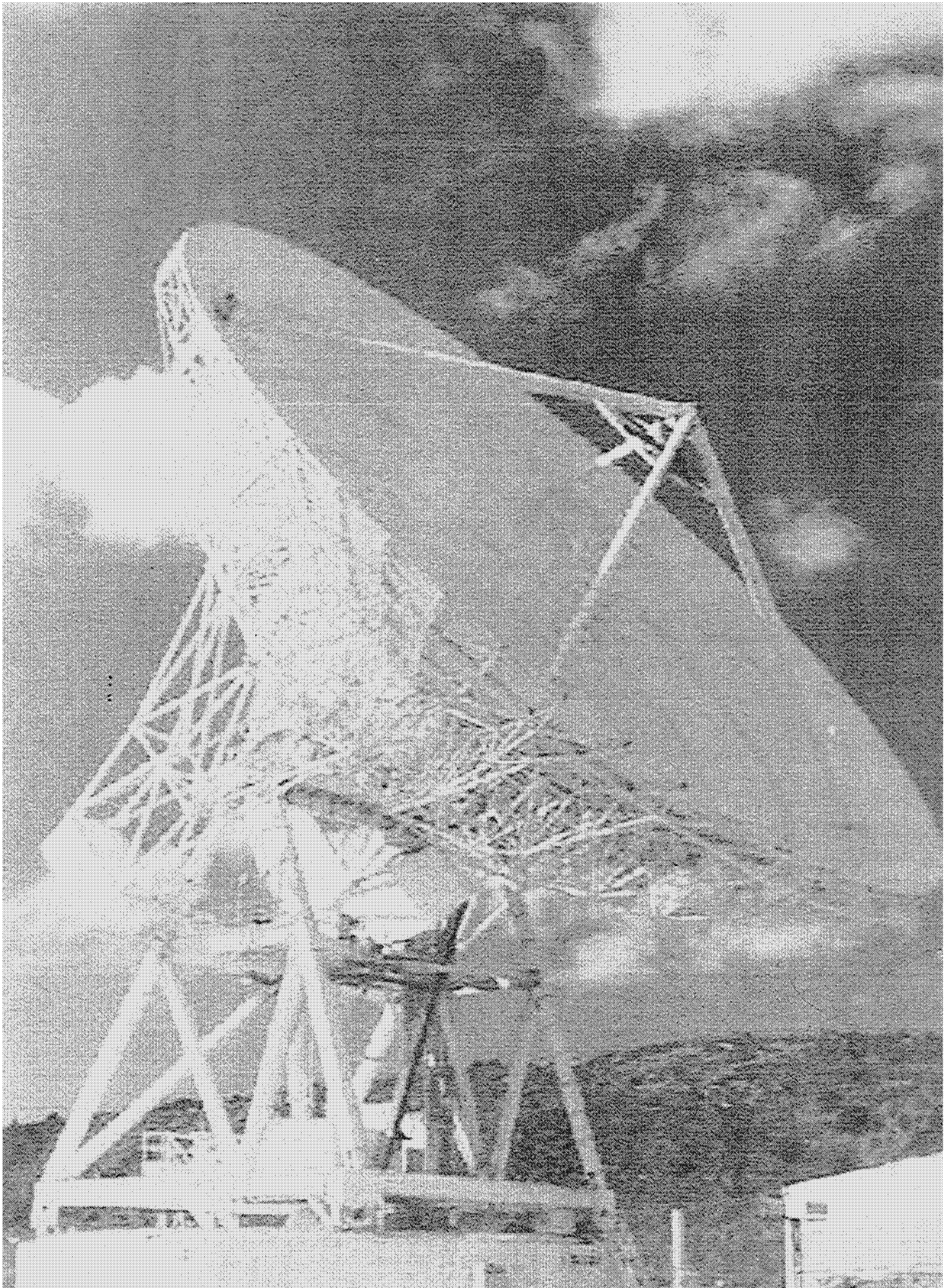
SOLAR WIND MAGNETIC FIELD

A-G98-114

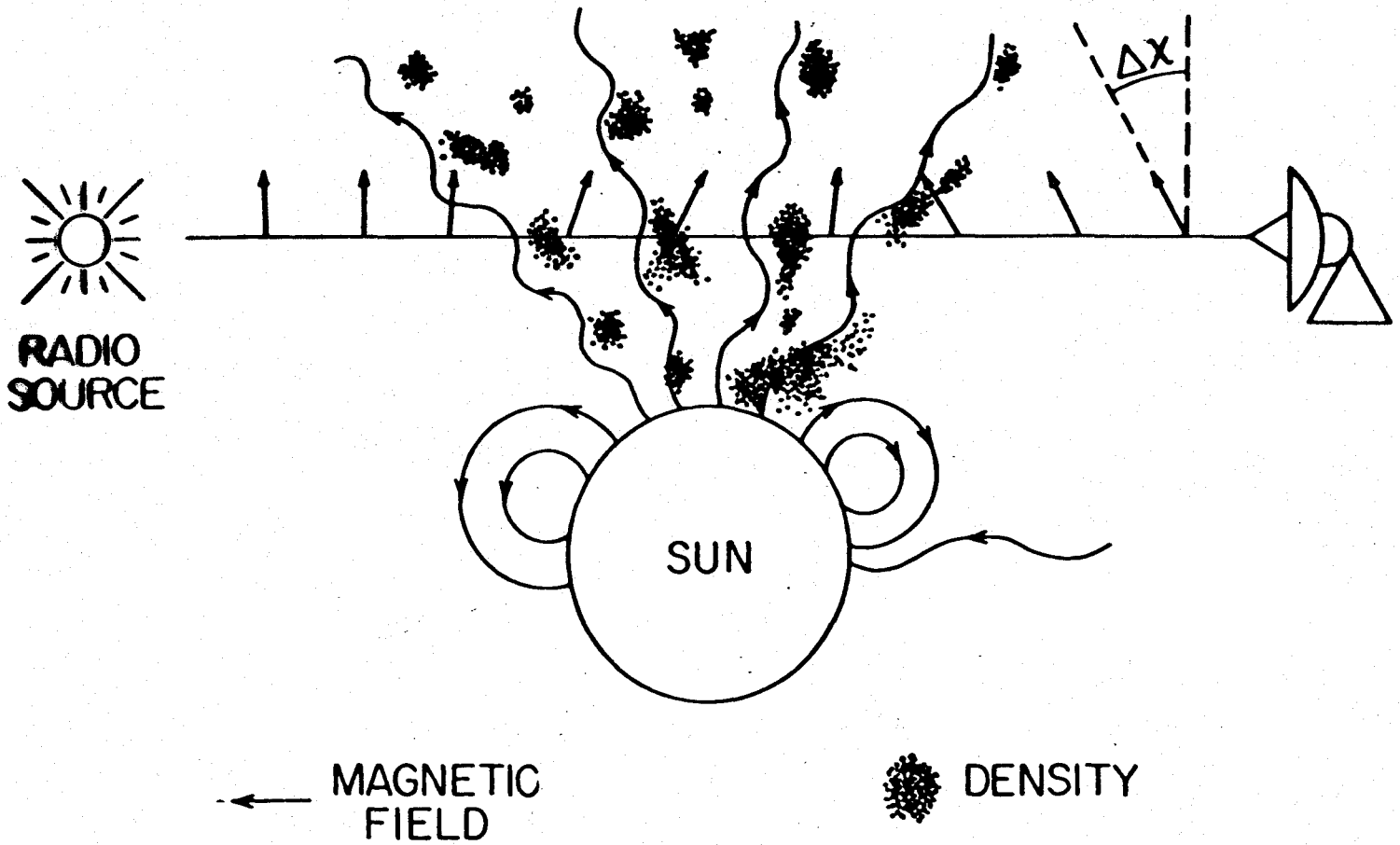


Roles of Astrophysical Turbulence

- Acceleration and transport of the cosmic rays
- Driving of fluid flows
- Support of molecular clouds against gravity
- Heating of the interstellar medium
- Transport of chemical inhomogeneities



CORONAL FARADAY ROTATION



$$\Delta X = \frac{e^3}{2\pi m_e^2 c^2 f^2} \int n_e \vec{B} \cdot d\vec{s}$$

The Physics of Faraday Rotation

The radio refractive index in a plasma

D. R. Nicholson, *Introduction to Plasma Theory* (1983)

$$n^2 = \frac{c^2}{v_p^2} = 1 - \frac{\omega_p^2}{\omega(\omega \pm \Omega_e)} \quad (1)$$

ω = wave frequency, ω_p = plasma frequency $\equiv \sqrt{\frac{4\pi n_e e^2}{m_e}}$, Ω_e = electron gyrofrequency $\equiv \frac{eB}{m_e c}$.

• Frequencies (f rather than ω) of observation typically 300 - 5000 MHz.

If $\Omega_e \ll \omega_p$,

$$n^2 = 1 - \frac{\omega_p^2}{\omega^2} \left(1 \mp \frac{\Omega_e}{\omega} \right) \quad (2)$$

For Low Density ISM (DIG) $\omega_p^2/\omega^2 \simeq 10^{-11}$, $\Omega_e/\omega \simeq 10^{-7}$.

$$v_p(RCP) = c - \frac{\omega_p^2}{2\omega^3} \Omega_e \quad (3)$$

$$v_p(LCP) = c + \frac{\omega_p^2}{2\omega^3} \Omega_e \quad (4)$$

Phase shift (centimeters) after traveling distance L

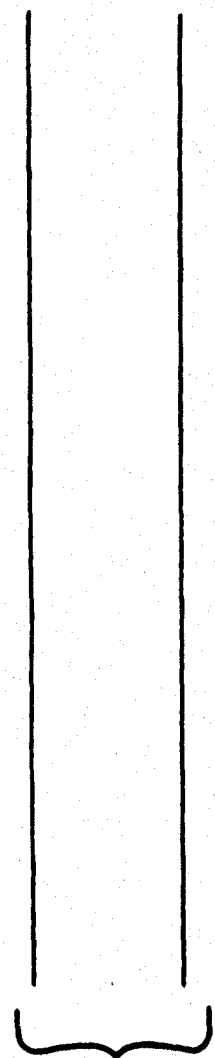
$$\Delta z = \left[\frac{e^3}{4\pi^2 m_e^2 c} \right] \frac{n_e B_z L}{f^3} \quad (5)$$

Phase shift in radians

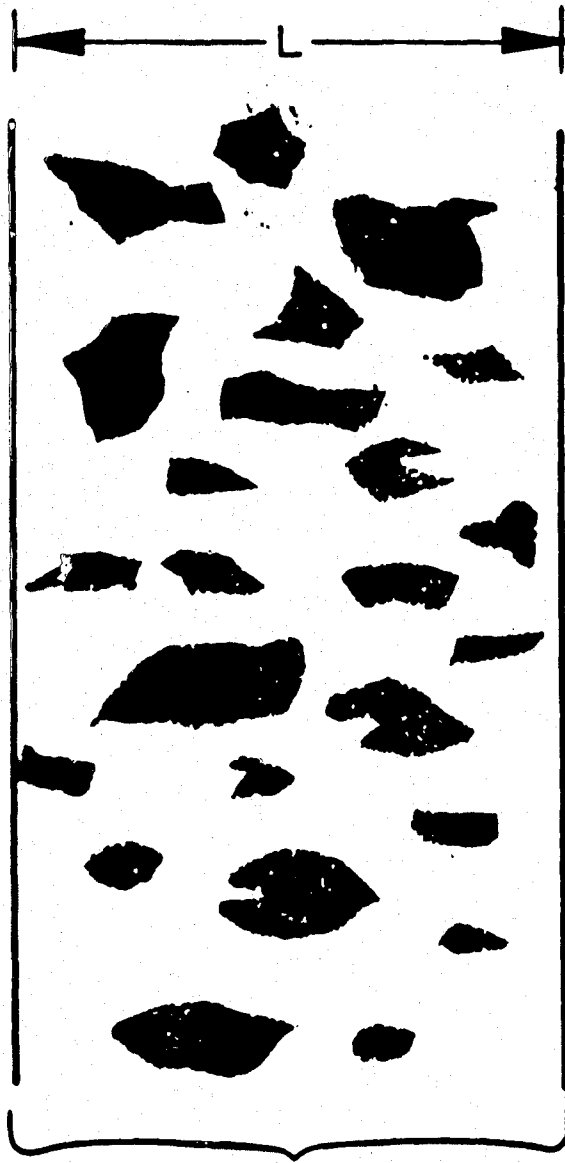
$$\Delta\phi = \frac{2\pi\Delta z}{\lambda} = \frac{e^3 n_e B_z L}{2\pi m_e^2 c^2 f^2} \quad (6)$$

$$\Delta\chi = \Delta\phi/2 = \frac{e^3 \lambda^2}{2\pi m_e^2 c^4} \int_L n_e \vec{B} \cdot \vec{ds} = 4.65^\circ \lambda^2 n_e B_z (\mu G) L_{kpc} \quad (7)$$

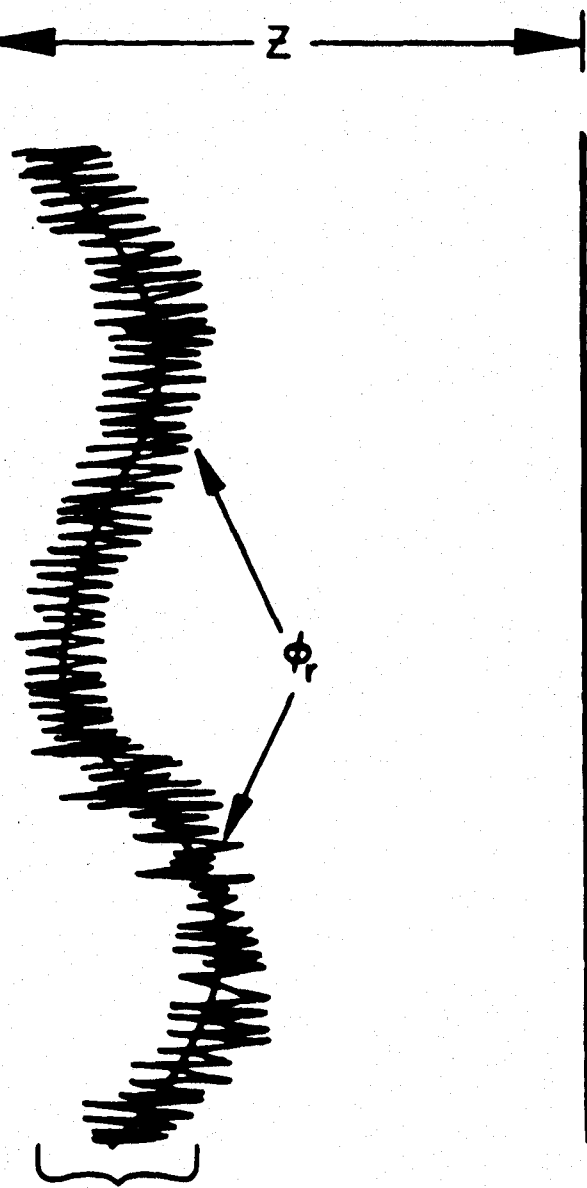
$\phi = \text{CONSTANT}$



PLANE WAVES



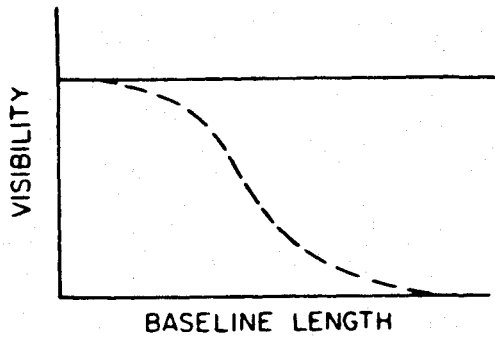
TURBULENT MEDIUM



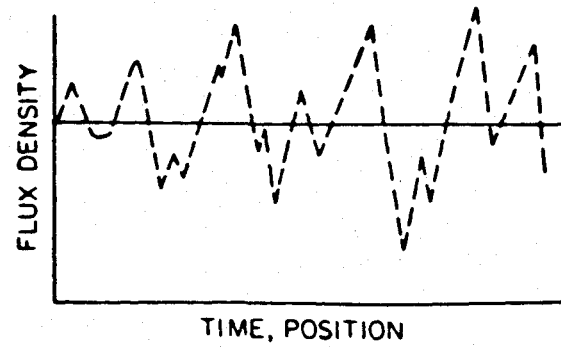
OBSERVER

INTERPLANETARY SCINTILLATION PHENOMENA

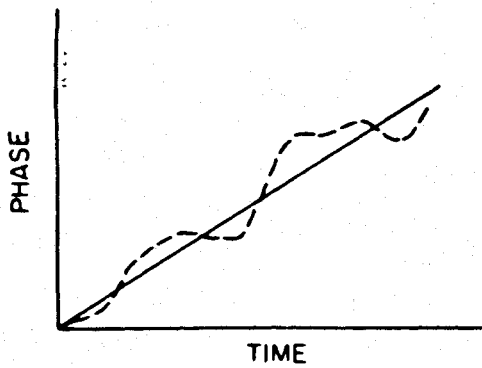
ANGULAR BROADENING



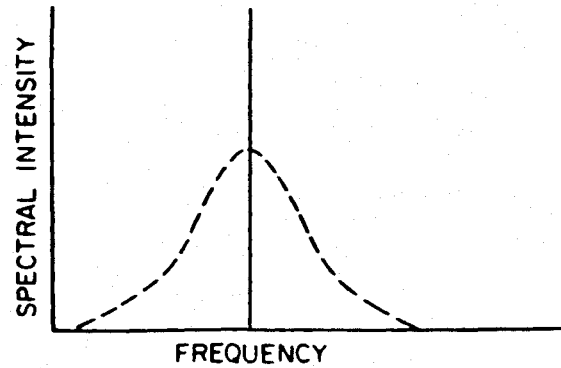
INTENSITY SCINTILLATIONS



PHASE SCINTILLATION



SPECTRAL BROADENING



————— WITHOUT TURBULENT MEDIUM
 - - - - - VIEWED THROUGH MEDIUM

- TIME-OF-ARRIVAL FLUCTUATIONS
- ROTATION MEASURE FLUCTUATIONS
- IMAGE DISTORTION AND WANDERING

1229+020 ON 9509:2 AT 93100 BOT-TOP KIRN SDKY

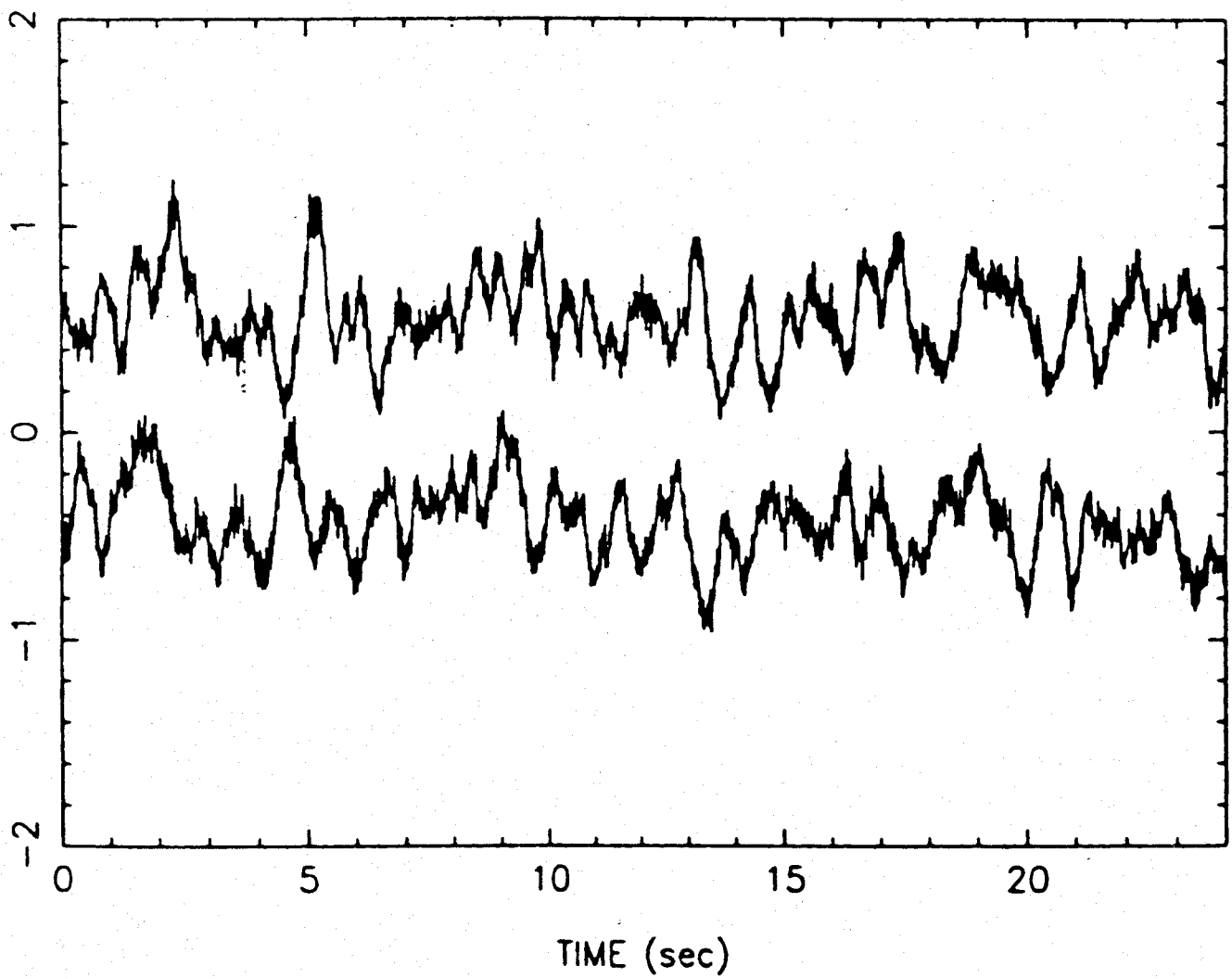


Figure 3.2 Time series of intensity.

Scintillations are a Stochastic Phenomenon

They yield information on statistical properties of the plasma turbulence density fluctuations

Exempli Causa... Refractive Scintillations

$$m^2 = 8\pi r_e^2 \lambda^2 \int_0^L dz \int_{-\infty}^{+\infty} d^2q P_{\delta n}(\vec{q}) \sin^2(q^2 z / 2k) |V(\vec{q}z/k)|^2 \quad (8)$$

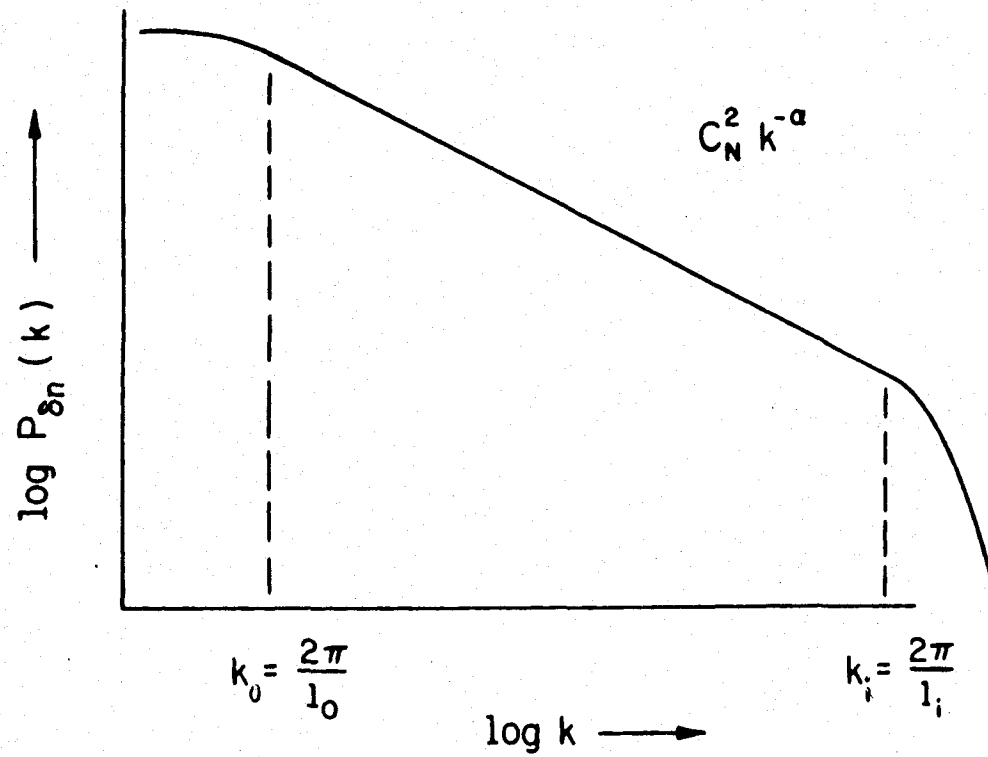
line of sight integral

density power spectrum

physics of scintillation process (Fresnel Filtering)

source characteristics (square of interferometric visibility)

INTERSTELLAR DENSITY POWER SPECTRUM



Fluid Turbulence: The Navier Stokes Equations

The Navier Stokes Equations

$$\frac{\partial \rho}{\partial t} + \nabla \cdot (\rho \vec{v}) = 0 \quad (1)$$

$$\frac{\partial \vec{v}}{\partial t} + (\vec{v} \cdot \nabla) \vec{v} = -\frac{1}{\rho} \nabla p + \nu \nabla^2 \vec{v} + \frac{1}{\rho} F_{ext} \quad (2)$$

$$\frac{\partial \epsilon}{\partial t} + \vec{v} \cdot \nabla \epsilon = -\frac{p}{\rho} \nabla \cdot \vec{v} + \frac{1}{\rho} \Lambda - \frac{1}{\rho} \nabla \cdot \vec{J} \quad (3)$$

In Turbulence

$$\rho = \bar{\rho} + \delta\rho, \quad \vec{v} = \bar{V} + \delta\vec{v}$$

$\delta\rho, \delta\vec{v}$ are stochastic parameters, describable in a statistical sense.

Astrophysical Fluids are Plasmas

Require use of Magnetohydrodynamic Equations

The Magnetohydrodynamic Equations

$$\Downarrow \frac{\partial \rho}{\partial t} + \nabla \cdot (\rho \vec{v}) = 0 \quad (4)$$

$$\frac{\partial \vec{v}}{\partial t} + (\vec{v} \cdot \nabla) \vec{v} = -\frac{1}{\rho} \nabla p + \frac{1}{\rho c} \vec{J} \times \vec{B} + \nu \nabla^2 \vec{v} + \frac{1}{\rho} F_{ext} \quad (5)$$

$$+ \text{Maxwell's Equations} \quad (6)$$

$$\frac{\partial \epsilon}{\partial t} + \vec{v} \cdot \nabla \epsilon = -\frac{p}{\rho} \nabla \cdot \vec{v} + \eta J^2 + \frac{1}{\rho} \Lambda - \frac{1}{\rho} \nabla \cdot \vec{J} \quad (7)$$

In Turbulence \Uparrow

$$\rho = \bar{\rho} + \delta\rho, \vec{v} = \bar{V} + \delta\vec{v}, \vec{B} = \bar{B}_0 + \delta\vec{b} \quad \text{⚡}$$

$\delta\rho, \delta\vec{v}, \delta\vec{b}$ are stochastic parameters, describable in a statistical sense.

Astrophysical Lighthill Radiation

MHD equations

$$\frac{\partial \rho}{\partial t} + \nabla \cdot (\rho \vec{v}) = 0 \quad (9)$$

$$\rho \frac{D\vec{v}}{Dt} = \frac{1}{c} \vec{J} \times \vec{B} - \nabla p \quad (10)$$

$$\vec{E} = -\frac{1}{c} \vec{v} \times \vec{B} \quad (11)$$

$$\nabla \times \vec{E} = -\frac{1}{c} \frac{\partial \vec{B}}{\partial t} \quad (12)$$

(one dimensional approximation) ↓

$$\frac{\partial^2 \rho}{\partial t^2} - c_s^2 \frac{\partial^2 \rho}{\partial z^2} = \frac{1}{2} \frac{\partial^2 b^2}{\partial z^2} + \frac{\partial^2 (\rho v_z^2)}{\partial z^2} \quad (13)$$

Fluctuations in b^2 and v generate fluctuations in density.

ISS sees the tip of a dynamical iceberg.

Both waves and hydroturbulence yield spatial gradients in b^2
and v .

The Utility of Radio Propagation Observations

Solar Wind

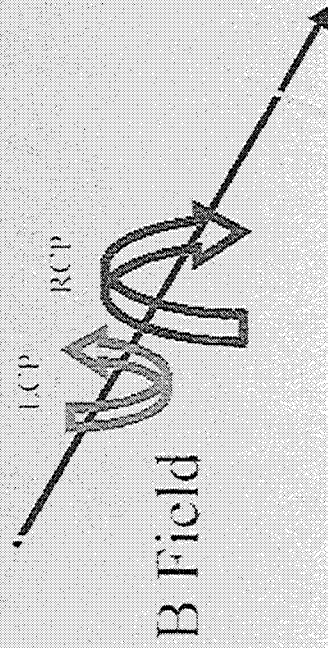
- Determine properties of solar wind plasma $\leq 60R_{\odot}$, particularly heliocentric distance dependence of turbulent intensity.
- Develop “ground truth” for radio remote sensing of plasma turbulence.

Interstellar Medium

- Provide guidance as to the equations to be used in theoretical studies of ISM turbulence (e.g. high degree of anisotropy in turbulence; $\delta n/n_0$).
- Provide indications as to solutions of these equations (e.g. power law spectra, possible existence of current sheets).

The Physics of Faraday Rotation

Faraday Rotation



Due to “Chirality” of medium
through which wave propagates

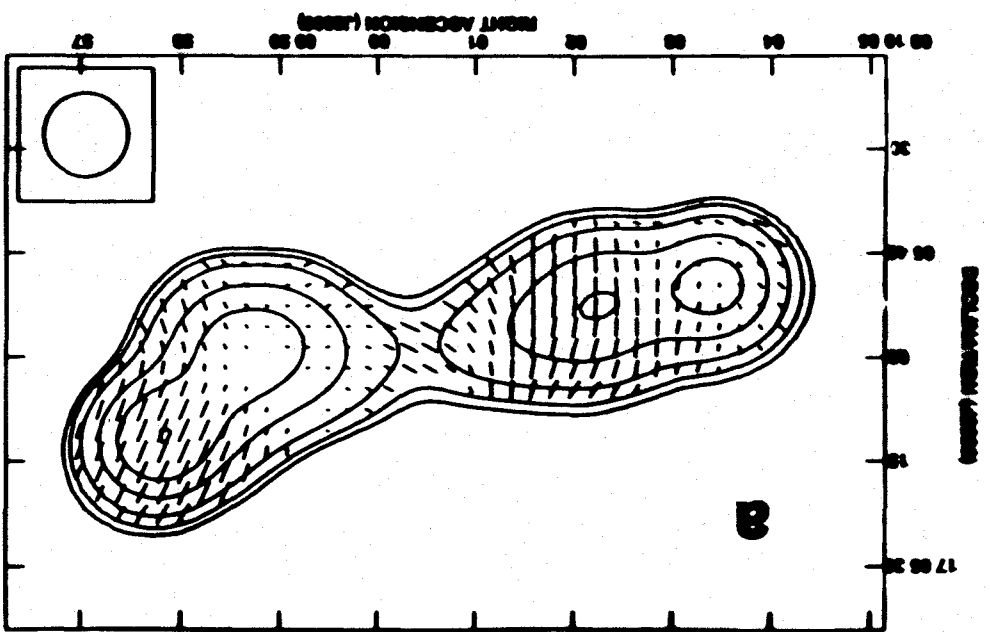
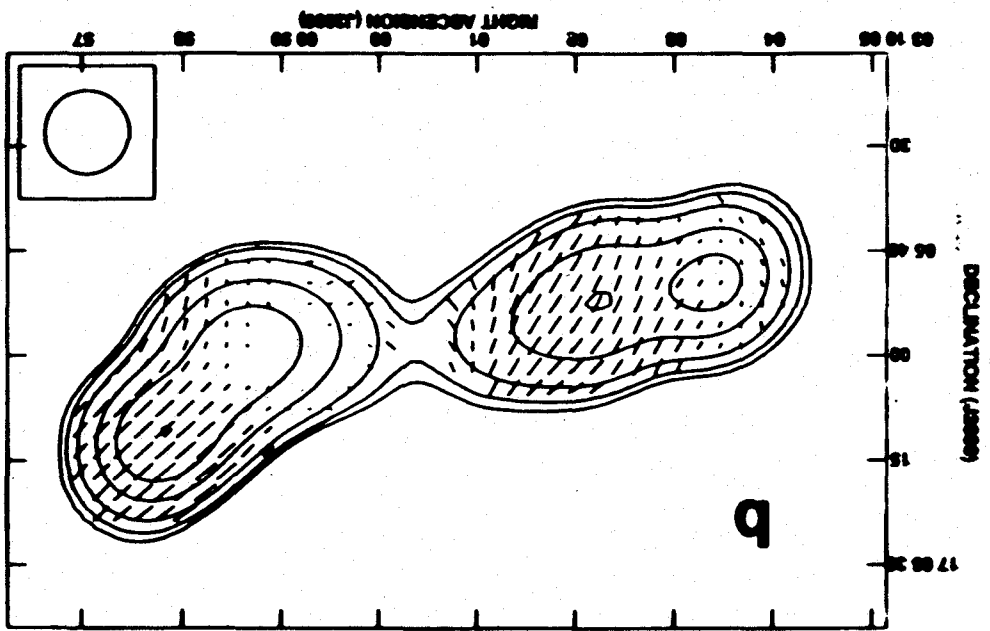
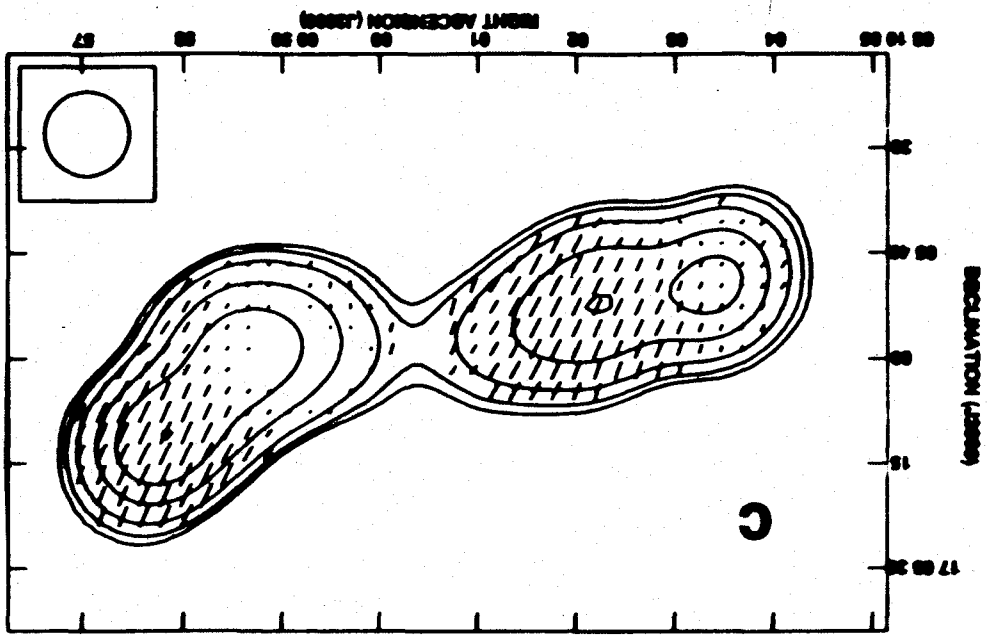
Faraday rotation is a rotation in the plane of polarization χ as a linearly polarized radio wave traverses a magnetized plasma.

$$\Delta\chi = \frac{e^3\lambda^2}{2\pi m_e^2 c^4} \int_L n_e \vec{B} \cdot d\vec{s} \quad (1)$$

In terms of units suitable for extragalactic radio sources,

$$\Delta\chi = 4.65^\circ \lambda^2 n_e B_z (\mu G) \bar{L}_{kpc} \quad (2)$$

\therefore A way of measuring δB
fluctuations on scales $\lambda \lesssim l_{out}$



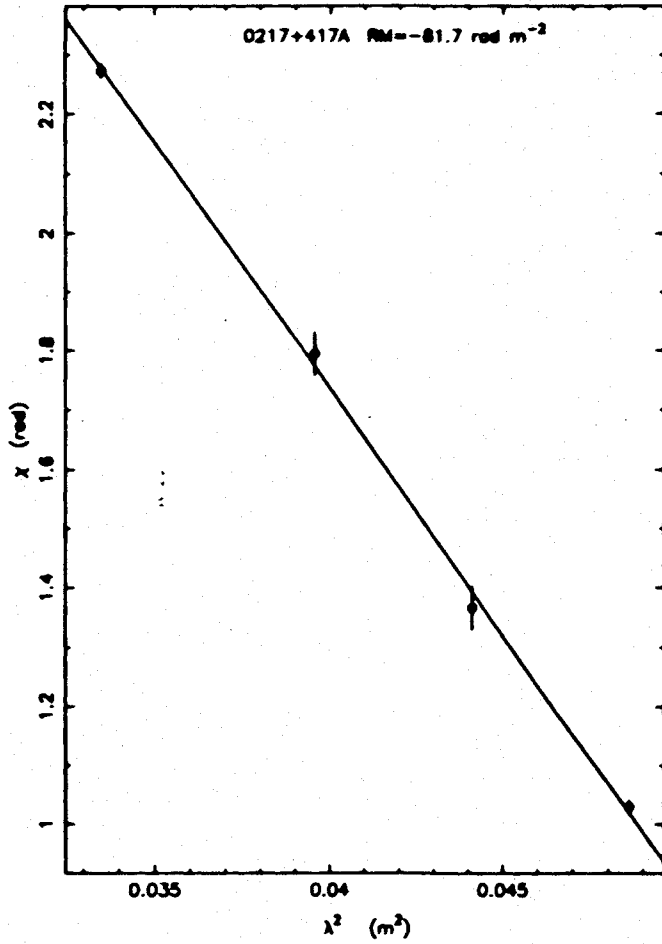


FIG. 2a

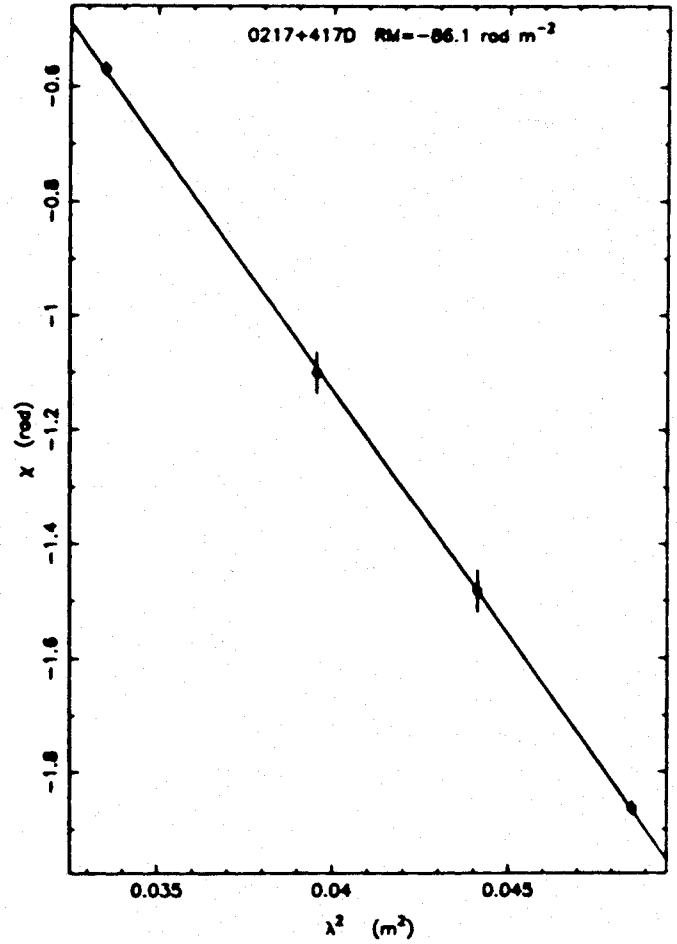


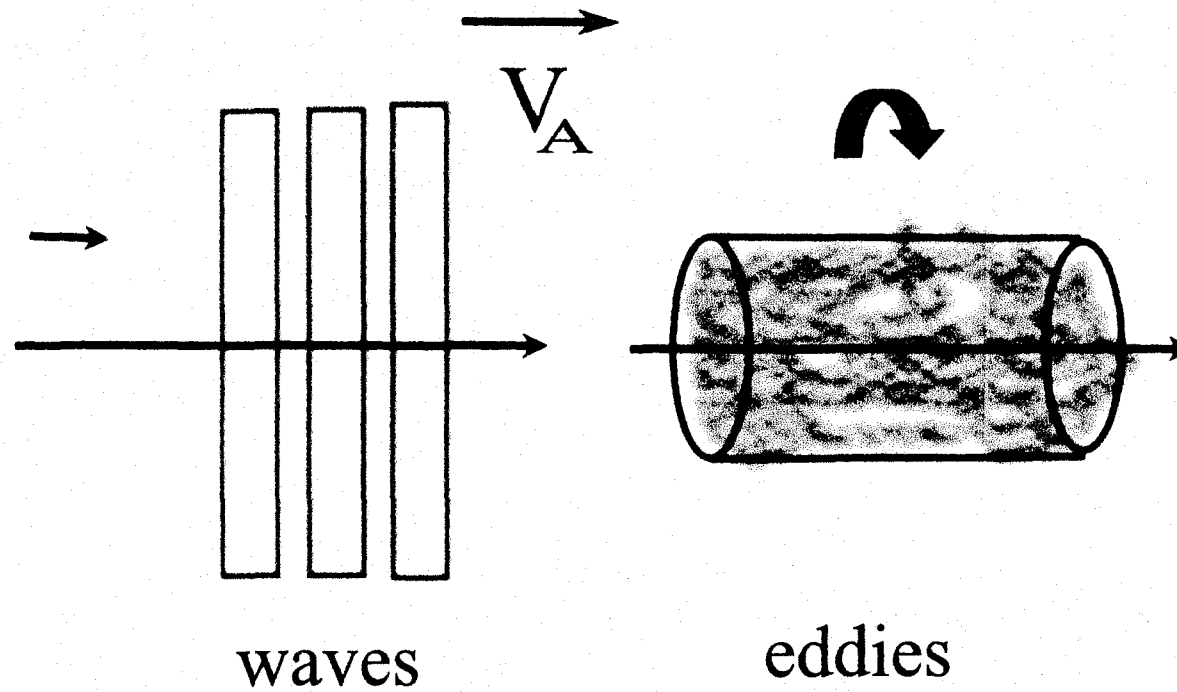
FIG. 2b

FIG. 2.—Fit of the rotation measure to the polarization position angles at the position of peak polarization intensity of the two lobes in 0217+417. The values of the least-squares fit rotation measure are $-81.7 \pm 0.6 \text{ rad m}^{-2}$ for component A, and $-86.1 \pm 1.2 \text{ rad m}^{-2}$ for component D.

Conclusions and Summary

- Turbulent density fluctuations produce stochastic radio wave propagation phenomena
- The scintillations effects are accurately measureable with existing radio telescopes
- The theory is well-developed to allow inference of density spectra
- Relation to other plasma variables still to be developed

Models of Magnetohydrodynamic Turbulence



10. MHD Turbulence in the Solar Wind

Eckart Marsch

10.1 Introduction

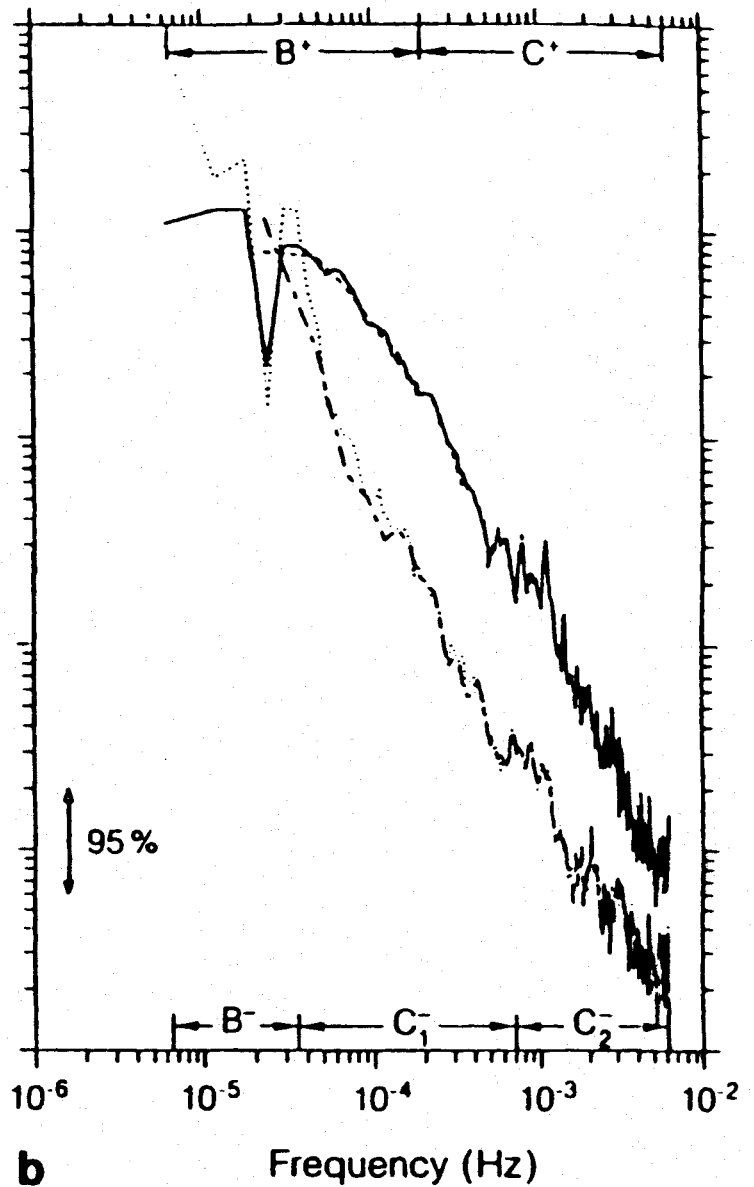
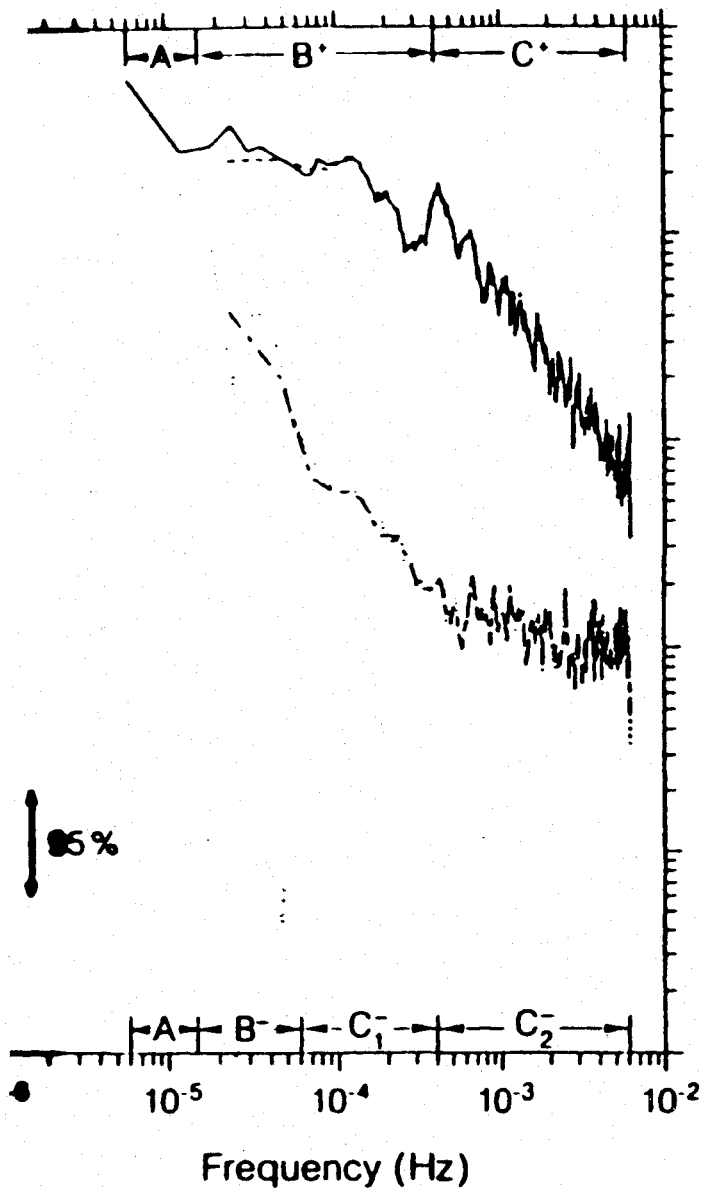
10.1.1 General and Historical Remarks

From the very beginning of *in situ* observations of the solar wind it was realized that the interplanetary medium by all appearances was usually not quiet but rather turbulent and visibly permeated by sizable fluctuations of the plasma flow velocity and density and of the magnetic field. Fluctuations occurred on all observed spatial and temporal scales, extending from the vast dimensions of the inner heliosphere and the corresponding solar wind transit time, or from the solar rotation period, down to the minute kinetic scales associated with the particles' gyromotion, where the dissipation was assumed finally to occur. The observational studies often revealed random and nonreproducible behavior of solar wind parameters as a function of time, thus indicating properties typical of a turbulent magnetofluid. The measured fractional variances of the magnetic field components, when normalized to the mean intensity, turned out to be large, suggesting the importance of nonlinear processes that couple a large number of degrees of freedom and turbulent "eddies" of disparate scales.

In a series of seminal papers Coleman [10.39–41] firmly established the turbulent character of solar wind fluctuations by showing that power-law spectra aptly fitted the data and that existing theoretical concepts, pertaining to the inertial range, as advanced by Kraichnan [10.93] seemed to be applicable. However, it also occurred some years later in studies that would have a similar impact on future research by Belcher and coworkers [10.19–21], that examples were found in the measurements of what resembled pure magnetohydrodynamic waves, notably Alfvén waves, stressing the possible persistence and coherence of the fluctuations.

Ever since, solar wind research has been perhaps somewhat misled by the fruitless controversy of "waves versus turbulence", which dominated interplanetary studies in the seventies and yielded many unsuccessful attempts to identify idealized wave properties in the data [10.3, 16, 44, 159]. In the past decade we have witnessed a period of new and fruitful approaches aimed at reconciling and unifying the two opposite points of view by means of modern concepts of magnetohydrodynamic turbulence, which provide valuable research tools for guiding solar wind studies, though they need to be adopted with caution, as discussed in detail in Montgomery's [10.128, 129] excellent survey of hydromagnetic tur-

Solar Wind Density Power Spectra



a Power spectra of Elsässer variables for high-speed (a) and low-speed (b) wind derived from data at 0.3 AU. Solid lines give e^+ and dotted lines e^- . The dashed and dot-dashed lines are derived by the Blackman-Tuckey technique. The error bar is based on a fit with 22 degrees of freedom [10.184]